Pathological Ace2-to-Ace enzyme switch in the stressed heart is transcriptionally controlled by the endothelial Brg1–FoxM1 complex

Jin Yang[a,b,c], Xuhui Feng[a,b,c], Qiong Zhou[a,b,c], Wei Cheng[a,b,c], Ching Shang[d], Pei Han[d], Chiou-Hong Lin[d], Huei-Sheng Vincent Chen[e], Thomas Quertermous[d], and Ching-Pin Chang[a,b,c,1]

[a]Krannert Institute of Cardiology and Division of Cardiology, Department of Medicine, Indiana University School of Medicine, Indianapolis, IN 46202; [b]Department of Biochemistry and Molecular Biology, Indiana University School of Medicine, Indianapolis, IN 46202; [c]Department of Medical and Molecular Genetics, Indiana University School of Medicine, Indianapolis, IN 46202; [d]Division of Cardiovascular Medicine, Stanford University School of Medicine, Stanford, CA 94305; and [e]Del E. Webb Neuroscience, Aging, and Stem Cell Research Center, Sanford/Burnham Medical Research Institute, La Jolla, CA 92037

Genes encoding angiotensin-converting enzymes (Ace and Ace2) are essential for heart function regulation. Cardiac stress enhances Ace, but suppresses Ace2, expression in the heart, leading to a net production of angiotensin II that promotes cardiac hypertrophy and fibrosis. The regulatory mechanism that underlies the Ace2-to-Ace pathological switch, however, is unknown. Here we report that the Brahma-related gene-1 (Brg1) chromatin remodeler and forkhead box M1 (FoxM1) transcription factor cooperate within cardiac (coronary) endothelial cells of pathologically stressed hearts to trigger the Ace2-to-Ace enzyme switch, angiotensin I-to-II conversion, and cardiac hypertrophy. In mice, cardiac stress activates the expression of Brg1 and FoxM1 in endothelial cells. Once activated, Brg1 and FoxM1 form a protein complex on Ace and Ace2 promoters to concurrently activate Ace and repress Ace2, tipping the balance to Ace2 expression with enhanced angiotensin II production, leading to cardiac hypertrophy and fibrosis. Disruption of endothelial Brg1 or FoxM1 or chemical inhibition of FoxM1 abolishes the stress-induced Ace2-to-Ace switch and protects the heart from pathological hypertrophy. In human hypertrophic hearts, BRG1 and FOXM1 expression is also activated in endothelial cells; their expression levels correlate strongly with the ACE/ACE2 ratio, suggesting a conserved mechanism. Our studies demonstrate a molecular interaction of Brg1 and FoxM1 and an endothelial mechanism of modulating Ace/Ace2 ratio for heart failure therapy.

chromatin remodeling | endothelial cells | Brg1 | FoxM1 | cardiac hypertrophy

Despite modern cardiac care, heart failure remains the leading cause of death, with a mortality rate of ~50% within 5 y of diagnosis (1). New mechanisms and therapeutic strategies for heart failure are needed. Most studies focus on the cardiomyocytes' maladaptive response to pathological stress as a cause of heart failure; little is known about how endothelial cells within the heart react to pathological stress to modify heart function. In heart failure patients without coronary artery disease, coronary endothelial dysfunction correlates with adverse cardiac remodeling, contractile abnormalities, and brain natriuretic peptide (BNP) levels (2–6); however, the endothelial function of peripheral arteries is preserved in those patients (3). These findings suggest that localized endothelial dysfunction in the heart is crucial for cardiac remodeling and hypertrophy. This aspect of cardiac endothelial function, however, is not well understood, and its clinical potential as a therapeutic target has not been sufficiently developed (7).

Heart function regulation requires angiotensin peptides (8), which are predominantly produced within the heart. Angiotensin peptides have much higher concentrations in the heart than in the plasma (9–11): The interstitial concentration of angiotensin II (Ang II) of the heart is ~100-fold more than that of plasma (11, 12). Within the heart, >90% of Ang I is synthesized locally, and >75%

of Ang II is produced by enzymatic conversion of the local cardiac Ang I (13, 14). Cardiac (coronary) endothelial cells are the primary source that produces angiotensin-converting enzymes (Ace and Ace2) to control angiotensin peptide production (8, 15). Ace and Ace2 are tethered to endothelial cell membrane or secreted into the interstitial space, where these enzymes process Ang I and II peptides. Biochemically, Ace converts the decapeptide Ang I (1–12) to octapeptide Ang II (1–10), whereas Ace2 degrades Ang II to form Ang-(1–7) (16) and cleaves Ang I into Ang-(1–9) (17). Functionally, Ang II is a potent stimulant of cardiac hypertrophy and fibrosis (8); conversely, Ang-(1–7) and Ang-(1–9) inhibit Ang II's cardiac effects to maintain heart function (8, 18). Therefore, Ace and Ace2 counteract each other to regulate heart function.

When the heart is pathologically stressed, Ace is up-regulated (19) and Ace2 down-regulated (20, 21), tipping the balance to Ace dominance with enhanced Ang II and reduced Ang-(1–7) and -(1–9) production. Such Ace/Ace2 perturbation contributes to the development of hypertrophy and heart failure. Inhibition of Ace (22) or overexpression of Ace2 protects the heart from stress-induced failure (20); conversely, Ace2 knockout mice exhibit heart dysfunction (23). Therefore, Ace promotes cardiac pathology (22), whereas Ace2 inhibits cardiomyopathy (20, 23). Balancing Ace/Ace2 is thus critical for maintaining heart function.

Significance

Angiotensin-converting enzymes Ace and Ace2 counteract each other to control the metabolism of angiotensin peptides and heart function. When the heart is pathologically stressed, Ace is up-regulated whereas Ace2 is down-regulated, leading to a pathological Ace2-to-Ace switch and increased production of angiotensin II, which promotes hypertrophy and fibrosis. The mechanism of Ace2-to-Ace switch is unknown. In this study, we discovered that the Ace/Ace2 switch occurs at the transcription level and defined a chromatin-based endothelial mechanism that triggers Ace/Ace2 transcription switch and heart failure. Human tissue studies suggest that this mechanism is evolutionarily conserved. Our studies reveal a pharmacological method to simultaneously inhibit pathogenic Ace and activate cardioprotective Ace2. This finding provides new insights and methods for heart failure therapy.

It is unclear how *Ace* and *Ace2* expression is controlled by endothelial cells within the heart. Gene regulation requires control at the level of chromatin, which provides a dynamic scaffold to package DNA and dictates accessibility of DNA sequence to transcription factors. Here we show that Brahma-related gene-1 (Brg1), an essential ATPase subunit of the BAF chromatin-remodeling complex (24), is activated by pathological stress within the endothelium of mouse hearts to control *Ace* and *Ace2* expression. Brg1 complexes with the forkhead box transcription factor forkhead box M1 (FoxM1), which has both transactivating and repressor domains for transcription regulation, to bind to *Ace* and *Ace2* promoters to simultaneously activate *Ace* and repress *Ace2* transcription. Mice with endothelial *Brg1* deletion or with FoxM1 inhibition or genetic disruption show resistance to stress-induced Ace/Ace2 switch, cardiac hypertrophy, and heart dysfunction. In human hypertrophic hearts, *BRG1* and *FOXM1* are also highly activated, and their activation correlates strongly with the ACE/ACE2 ratio and disease severity, indicating a conserved endothelial mechanism for human cardiomyopathy. Brg1 and FoxM1 are therefore essential endothelial mediators of cardiac stress that triggers pathological hypertrophy. Given the lack of ACE2 drugs that limit full clinical exploitation of this pathway, targeting the Brg1–FoxM1 complex may offer an alternative strategy for concurrent ACE and ACE2 control in heart failure therapy. Furthermore, the studies demonstrated a molecular interaction between Brg1 and FoxM1 in gene control, which provides novel insights into the mechanisms of FoxM1-mediated organ development and oncogenic processes (25–27).

Results

Dynamic Changes of Endothelial Factors that Contribute to Cardiac Hypertrophy. To identify endothelial factors that might contribute to cardiomyopathy, we surveyed a number of endothelial genes for their changes of expression after left ventricular pressure overload generated by transaortic constriction (TAC) (24, 28). TAC-induced heart dysfunction was verified by echocardiography and molecular markers *Myh6*, *Myh7*, *Anf*, *Bnp*, and *Serca2a* (Figs. S1 *A and B* and S2 *A–D*). By performing reverse transcription and quantitative PCR (RT-qPCR) of left ventricles (LVs), we examined the expression of the following cardiac endothelial factors with or without TAC: *eNos*, *Et-1*, *Adamts1*, *Hdac7*, *Nrg1*, *Ace*, and *Ace2* (29). Within 7 d after TAC, *Et-1* and *Ace* were induced 2.0- and 2.1-fold in LVs, whereas *Enos* and *Ace2* were reduced by 46% and 43%, respectively (Fig. 1*A*). *Adamts1*, *Hdac7*, and *Nrg1* had no significant changes.

Given that *Ace* and *Ace2* encode enzymes that are critical for heart function (20–23, 29), we focused on the control of *Ace* and *Ace2* expression in TAC-stressed hearts. Immunostaining showed that Ace proteins were present at low levels in healthy hearts, but up-regulated in the endothelium of stressed hearts (Fig. 1 *B* and *C* and Fig. S1 *C* and *D*). In contrast, Ace2 proteins were present at high levels in the endothelium of healthy hearts, but down-regulated in TAC-stressed hearts (Fig. 1 *D* and *E*). To further verify the opposite changes of Ace and Ace2 in endothelial cells, we used anti-CD31 magnetic beads to isolate endothelial cells from hearts after 7 d of sham or TAC operation (30) (Fig. S1 *E* and *F*). Immunostaining with anti-CD31/Pecam showed that endothelial cells constituted >90% of the sorted cells (Fig. S1 *E* and *F*). Western blot analysis confirmed that Ace proteins were up-regulated to 2.0-fold and Ace2 proteins reduced by 46%, with the ratio of Ace/Ace2 proteins changed by 3.7-fold in endothelial cells of the stressed hearts (Fig. 1 *H* and *I*). Such Ace and Ace2 misregulation was also present after 2 and 4 wk of TAC (Fig. S2).

With the view that Ace is known to promote cardiac pathology (22), whereas Ace2 inhibits cardiomyopathy (20, 23), such opposite expression dynamics indicates that a loss of balance between Ace and Ace2 in pressure-stressed hearts is crucial for the development of pathological hypertrophy. Furthermore, the magnitude
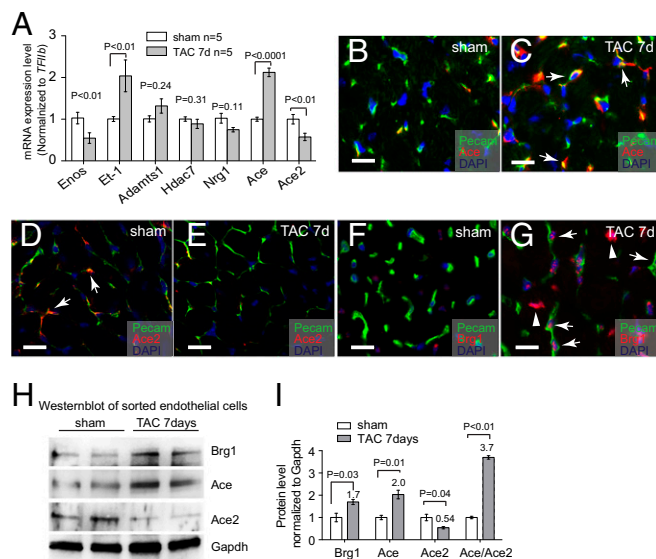

Fig. 1. Stress-induced changes of endothelial Ace, Ace2, and Brg1 in the hearts. (*A*) qRT-PCR analysis of *eNos*, *Et-1*, *Adamts1*, *Hdac7*, *Nrg1*, *Ace*, and *Ace2* in the mice heart ventricles after sham or TAC operation. *n* = 5 mice per group. *P* value: Student's *t* test. Error bar: SEM. (*B* and *C*) Coimmunostaining of Ace (red, arrows) and Pecam (green, labeling endothelial cells) in left ventricles 7 d after sham (*B*) or TAC (*C*) operation. Blue, DAPI nuclear stain. (Scale bars, 10 μm.) (*D* and *E*) Coimmunostaining of Ace2 (red, arrows) and Pecam (green, labeling endothelial cells) in left ventricles 7 d after sham (*D*) or TAC (*E*) operation. Blue, DAPI nuclear stain. (Scale bars, 10 μm.) (*F* and *G*) Coimmunostaining of Brg1 (red) and Pecam (green, labeling endothelial cells) in left ventricles 7 d after sham (*F*) or TAC (*G*) operation. Blue, DAPI nuclear stain. Arrows, Brg1 in endothelial cell nuclei; arrowheads, Brg1 in myocardial cell nuclei. (Scale bars, 10 μm.) (*H* and *I*) Western blot analysis (*H*) and quantitation (*I*) of Ace, Ace2, and Brg1 proteins in cardiac endothelial cells isolated from mouse hearts 7 d after sham or TAC operation. *P* value: Student's *t* test. Error bar: SEM.

of stress-induced changes in Ace and Ace2 proteins was comparable to that of mRNA (Fig. 1 *A* and *I*), indicating that the primary regulation of Ace and Ace2 in stressed hearts occurs at the transcription level.

Endothelial Brg1 Is Essential for Cardiac Hypertrophy and Dysfunction. Given that gene-transcription control requires chromatin regulation and that the chromatin remodeler Brg1 is known to control the pathological *Myh6/Myh7* switch in stressed cardiomyocytes (24, 28), we hypothesized that Brg1, like in the control of the *Myh6/Myh7* switch, could function in endothelial cells to control the *Ace/Ace2* switch in stressed hearts. Immunostaining showed that Brg1 was expressed at a minimal/low level in endothelial cells of healthy adult hearts. However, when the hearts were stressed by TAC, Brg1 was up-regulated in the nuclei of both cardiomyocytes and endothelial cells (Fig. 1 *G* and *I*). To compare Brg1 expression in cardiomyocytes and endothelial cells, we isolated these two types of cells from sham or TAC-stressed hearts (30) (Figs. S1 *E* and *F* and S3*A*). We found comparable changes of Brg1 expression in those two cell types. TAC increased Brg1 mRNA by ~1.6-fold and Brg1 protein by twofold in both cardiomyocytes and endothelial cells (Fig. S3 *B–D*). Although Brg1 activation in cardiomyocytes is crucial for the development of cardiac hypertrophy (24, 28), the function of Brg1 in the endothelium of hypertrophic hearts was unknown.

To test the role of endothelial Brg1 in stressed hearts, we used a tamoxifen-inducible *SclCre^{ERT}* mouse line (31) to induce endothelial *Brg1* deletion in mice that carried floxed alleles of the *Brg1* gene (*Brg1^{fl}*) (32). Immunostaining showed that tamoxifen treatment for 5 d (0.1 mg per gram of body weight, oral gavage once every other day, three doses total) before the TAC surgery was

sufficient to activate a β-galactosidase reporter (R26R) and to disrupt Brg1 expression in endothelial cells, but not cardiomyocytes, of TAC-stressed hearts (Fig. 2 *A–D*). We then used TAC to pressure-overload the heart and induce hypertrophy in littermate control ($SclCre^{ER}; Brg1^{fl/+}$ or $Brg1^{fl/fl}$) and mutant $SclCre^{ERT}; Brg1^{fl/fl}$ mice with or without tamoxifen treatment. Left ventricular fractional shortening (FS) changes were followed by echocardiography (Fig. S4*A*). Four weeks after TAC, the control mice developed larger hearts than those of $SclCre^{ER}; Brg1^{fl/fl}$ mice lacking endothelial Brg1 (Fig. 2*E*). Analysis of the cardiac mass (ventricle–body weight ratio) showed an ~50% reduction of hypertrophy (from 77% to 41%) in $SclCre^{ERT}; Brg1^{fl/fl}$ mice (Fig. 2*F*). Cell size measurement by wheat germ agglutinin (WGA) staining revealed ~70% reduction of cardiomyocyte size (from 74% to 21%) in $SclCre^{ERT}; Brg1^{fl/fl}$ mice (Fig. 2*G* and Fig. S4 *B–E*). There was also a dramatic reduction of interstitial fibrosis in the $SclCre^{ERT}; Brg1^{fl/fl}$ mice (Fig. 2 *H* and *I*). Within 4 wk after TAC, $SclCre^{ERT}; Brg1^{fl/fl}$ mice showed 23% improvement of left ventricular FS ($P < 0.01$; Fig. 2*J* and Fig. S4*A*).

To further determine cardiac function, we inserted a catheter from the right carotid artery retrograde into the LV to measure its pressure and volume (Fig. 2*K*). The in vivo catheterization showed that TAC increased the peak LV systolic pressure from 100 to 150 mmHg (Fig. 2*K*), with a peak pressure overload of ~50 mmHg. This LV pressure overload was comparable between the control and mutant hearts (Fig. 2*L*). The peripheral systolic pressure (right carotid artery) was identical to that of LV and had no difference between control and mutant mice. Endothelial *Brg1* deletion greatly improved the function of TAC-stressed hearts. $SclCre^{ERT};$ $Brg1^{fl/fl}$ mice exhibited much better cardiac function 4 wk after TAC. Ejection fraction (EF) improved by 49% ($P < 0.001$) (Fig. 2*M*); preload-adjusted maximal power (plPwr) by 38% ($P = 0.04$) (Fig. 2*N*); stroke volume (SV) by 35% ($P = 0.02$) (Fig. 2*O*); and stroke work (SW) by 20% ($P = 0.03$) (Fig. 2*P*). Also, $SclCre^{ERT};$ $Brg1^{fl/fl}$ mice had less dilated hearts, with end-systolic volume (ESV) reduced by 32% ($P < 0.01$) (Fig. 2*Q*) and end-diastolic volume (EDV) reduced by 15% ($P = 0.02$) and normalized (Fig. 2*R*). Both the LV contractility and volume measurement indicate a major improvement in systolic function of the heart. Furthermore, $SclCre^{ERT}; Brg1^{fl/fl}$ hearts had greatly improved diastolic function. This result was evidenced by the reduction of isovolumic relaxation time constant tau by 42.3% ($P = 0.01$) (Fig. 2*S*) and end-diastolic pressure (EDP) by 21% ($P = 0.03$) (Fig. 2*T*). As a result of systolic and diastolic functional improvement, $SclCre^{ERT}; Brg1^{fl/fl}$ mice showed a 33% ($P = 0.02$) increase of cardiac output (CO) (Fig. 2*U*). Consistent with the functional improvement of TAC-operated $SclCre^{ERT}; Brg1^{fl/fl}$ mice, molecular markers *Myh6* and *Serca2a* were significantly increased, whereas the stress markers *Myh7*, *Anf*, and *Bnp* were much reduced (Fig. S4*F*). This result is consistent with the resistance of $SclCre^{ERT}; Brg1^{fl/fl}$ to TAC-induced heart failure. Overall, endothelial *Brg1*-null mice had a 50–70% reduction of cardiac hypertrophy, minimal/absent interstitial fibrosis, and reduction of heart functional decline after TAC. These findings indicate that the Brg1 is activated by stress in cardiac endothelial cells to trigger hypertrophy.

Endothelial Brg1 Controls *Ace*/*Ace2* Expression and Ang I/II Metabolism. Given that defective angiogenesis might contribute to cardiac hypertrophy and failure (33), we examined cardiac vessel density to test whether endothelial Brg1 was essential for angiogenesis in stressed hearts. By Pecam staining, we found no difference in vascular density of control and $SclCre^{ERT}; Brg1^{fl/fl}$ hearts treated with tamoxifen and TAC (Fig. S5 *A–E*).

We then tested whether endothelial Brg1 controlled changes of Ace and Ace2 in stressed hearts. By RT-qPCR of heart ventricles, we examined the expression of *eNos*, *Et1*, *Adamts1*, *Hdac7*, *Nrg1*, *Ace*, and *Ace2* in tamoxifen-treated control and $SclCre^{ERT}; Brg1^{fl/fl}$ hearts with or without TAC. Among these genes and after TAC, the stress-induced opposite changes of *Ace* and *Ace2* were evident
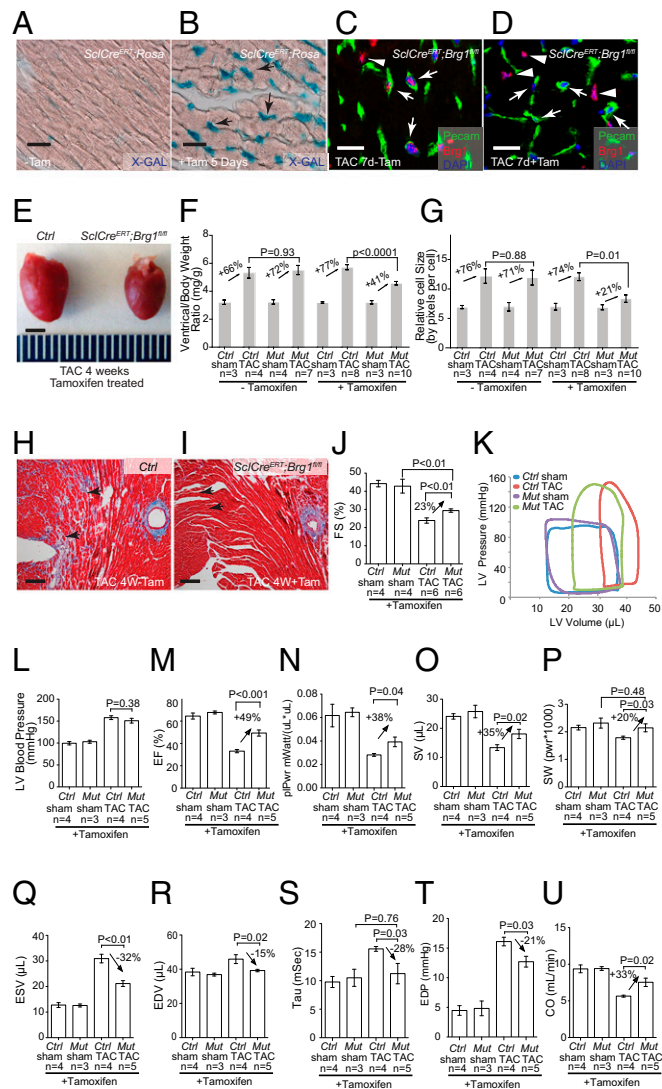

Fig. 2. Endothelial Brg1 is essential for stress-induced cardiac hypertrophy and dysfunction. (*A* and *B*) β-galactosidase (X-gal) staining (blue) of $SclCre^{ERT};$ *R26R* mouse hearts without (*A*) or with (*B*) 5 d of tamoxifen (Tam) treatment. Arrow, endothelial cells. (Scale bar, 10 μm.) (*C* and *D*) Coimmunostaining of Brg1 (red) and Pecam (green, labeling endothelial cells) in $SclCre^{ERT}; Brg1^{fl/fl}$ hearts 7 d after TAC without (*C*) or with (*D*) 5-d tamoxifen treatment. Blue, DAPI nuclear stain. Arrows, endothelial cell nuclei; arrowheads, myocardial cell nuclei. (Scale bars, 10 μm.) (*E*) Gross picture of hearts harvested 4 wk after sham or TAC operation in control and $SclCre^{ERT}; Brg1^{fl/fl}$ mice treated with tamoxifen. (Scale bar, 2 mm.) (*F*) Quantitation of ventricle–body weight ratio in control (Ctrl) and $SclCre^{ERT}; Brg1^{fl/fl}$ (Mut) mice 4 wk after sham or TAC operation. *P* value: Student's *t* test. Error bar: SEM. (*G*) Quantitation of cardiomyocyte size by wheat germ agglutinin (WGA) staining in control and $SclCre^{ERT}; Brg1^{fl/fl}$ mice 4 wk after sham or TAC operation. (*H* and *I*) Trichrome staining of cardiac fibrosis in control (*H*) and $SclCre^{ERT}; Brg1^{fl/fl}$ (*I*) mice 4 wk after TAC operation. Red, cardiomyocytes; blue, fibrosis. Arrows, interstitial space. (Scale bars, 50 μm.) (*J*) Echocardiographic measurement of fractional shortening (FS) of the left ventricle after 4 wk of TAC. (*K*) Representative left ventricular (LV) pressure–volume (PV) loops taken after cardiac catheterization of control (Ctrl) and $SclCre^{ERT};$ $Brg1^{fl/fl}$ (Mut) mice 4 wk after sham or TAC operation. (*L–P*) Quantitation of left ventricular systolic pressure (*L*), ejection fraction (EF; *M*), preload-adjusted maximal power (plPwr; *N*), stroke volume (SV; *O*), and stroke work (SW; *P*) 4 wk after sham or TAC operation. Ctrl, control mice; Mut, $SclCre^{ERT};$ $Brg1^{fl/fl}$ mice. (*Q–U*) Quantitation of end-systolic volume (ESV; *Q*), end-diastolic volume (EDV; *R*), Tau (*S*), end-diastolic pressure (EDP; *T*), and cardiac output (CO; *U*) 4 wk after sham or TAC operation. Ctrl, control mice; Mut, $SclCre^{ERT};$ $Brg1^{fl/fl}$ mice.

in the control mice, with TAC increasing Ace/Ace2 ratio by 4.3-fold (Fig. 3*A*). However, such Ace/Ace2 changes were eliminated in the TAC-stressed hearts of *SclCre*[ERT]*;Brg1*^{fl/fl} mice (Fig. 3*A* and Fig. S5 *F and G*), indicating that endothelial Brg1 is essential for *Ace* up-regulation and *Ace2* down-regulation in stressed hearts. In contrast, the changes of other endothelial genes (*eNos*, *Et1*, *Adamts1*, *Hdac7*, and *Nrg1*) were not affected by endothelial Brg1 (Fig. S5*H*). These data suggest a degree of Brg1 specificity in control of the Ace/Ace2 switch. Consistently, immunostaining showed that Brg1 was required for the pathological switch of Ace and Ace2 proteins in the heart endothelium. TAC-induced Ace protein up-regulation and Ace2 down-regulation were essentially abolished in the *SclCre*[ERT]*;Brg1*^{fl/fl} hearts (Fig. 3 *B–I*). These findings were confirmed by Western blot quantitation of Ace and Ace2 in heart protein extracts from the control and mutant mice (Fig. 3 *J* and *K*). Furthermore, consistent with the Brg1-mediated control of the Ace/Ace2 ratio, the TAC-induced Ang I reduction

and Ang II increase was present in the control hearts, but reversed in the mutant *SclCre*[ERT]*;Brg1*^{fl/fl} hearts (Fig. 3*L*). Also, despite the cardiac changes of angiotensin, Brg1 mutation caused no change of Ang II in the plasma (Fig. 3*M*). These findings are consistent with cardiac Ang I and II being primarily produced locally (11–14) and that such local angiotensin production is regulated by cardiac endothelial Brg1. Collectively, the results indicate that endothelial Brg1 responds to cardiac stress to activate *Ace* and repress *Ace2* expression, triggering a pathological switch of Ace and Ace2 in stressed hearts.

Brg1 Binds to the Promoters of *Ace* and *Ace2* to Regulate Their Expression. To determine whether Brg1 directly regulated *Ace* and *Ace2* expression in the stressed hearts, we first examined the binding of Brg1 to *Ace* and *Ace2* promoters. With sequence alignment, we identified four regions (a1–a4) in the ~3-Kb upstream region of the mouse *Ace* promoter that are evolutionarily conserved in mouse, rat, and human (Fig. 3*N*). Chromatin immunoprecipitation (ChIP) assay using
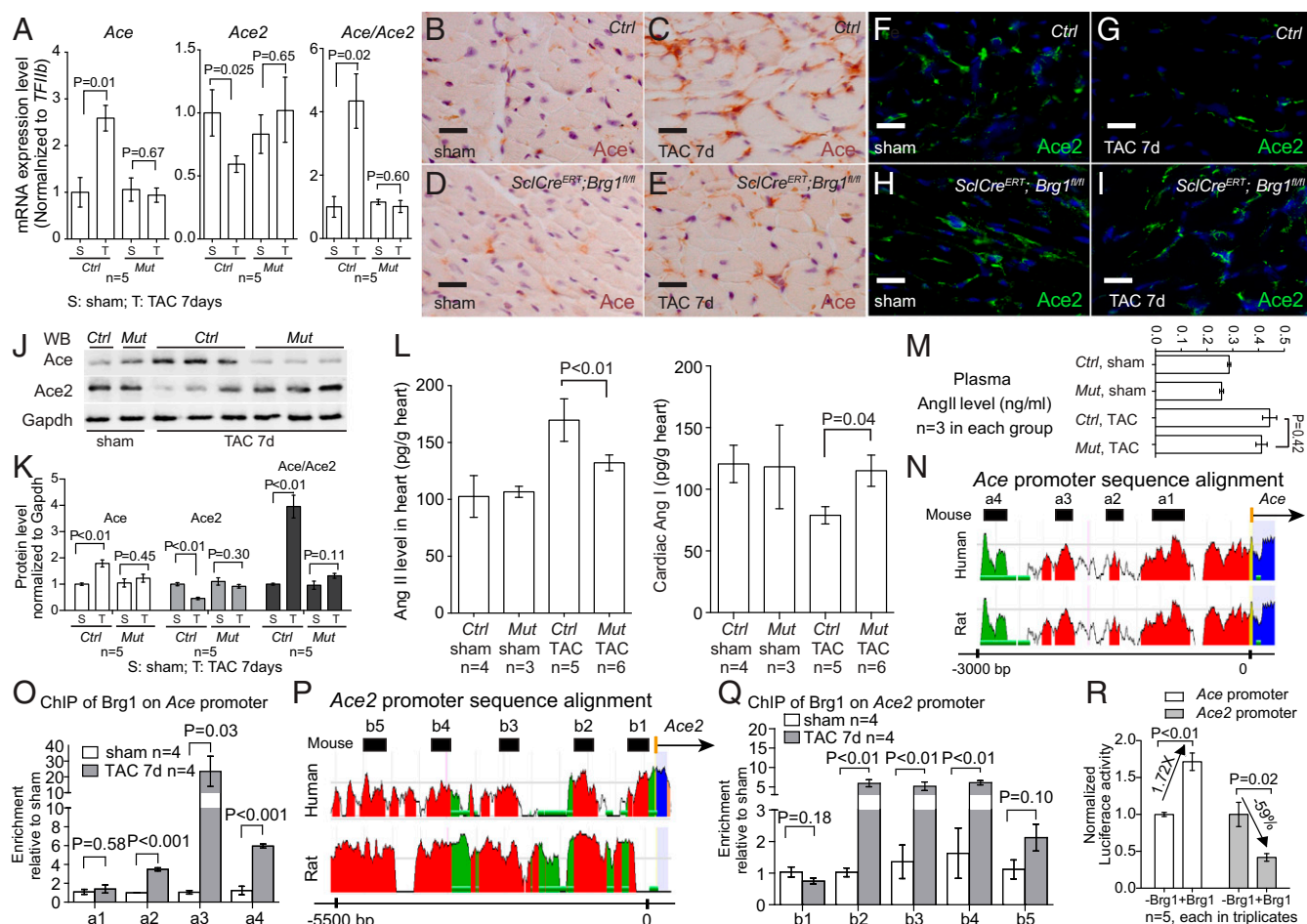

Fig. 3. Endothelial Brg1 controls *Ace*/*Ace2* expression and Ang I/II metabolism in stressed hearts. (*A*) Quantitation of *Ace*, *Ace2*, and *Ace/Ace2* in control (Ctrl) and *SclCre*[ERT]*;Brg1*^{fl/fl} (Mut) hearts after 7 d of sham or TAC operation. (*B–E*) Immunostaining of Ace (brown) in control (*B* and *C*) and *SclCre*[ERT]*;Brg1*^{fl/fl} (*D* and *E*) hearts 7 d after sham or TAC operation. (Scale bars, 10 μm.) (*F–I*) Immunostaining of Ace2 (green) in control (*F* and *G*) and *SclCre*[ERT]*;Brg1*^{fl/fl} (*H* and *I*) hearts 7 d after sham or TAC operation. (Scale bars, 10 μm.) (*J* and *K*) Western blot analysis (*J*) and quantitation (*K*) of Ace and Ace2 proteins in control (Ctrl) and *SclCre*[ERT]*; Brg1*^{fl/fl} (Mut) hearts 7 d after sham or TAC operation. *P* value: Student's *t* test. Error bar: SEM. (*L* and *M*) ELISA analysis of Ang I and II concentrations in the heart (*L*) and plasma (*M*) 4 wk after TAC. Ctrl, control; Mut, *SclCre*[ERT]*;Brg1*^{fl/fl}. *P* value: Student's *t* test. Error bar: SEM. (*N*) Sequence alignment of the *Ace* locus from mouse, human, and rat. Peak heights indicate degree of sequence homology. Black boxes (a1–a4) are regions of high sequence homology and were further analyzed by ChIP. Red, promoter elements; yellow, untranslated regions; green, transposons/simple repeats. (*O*) ChIP-qPCR analysis of *Ace* promoter using antibodies against Brg1 (J1 antibody) and hearts 7 d after sham or TAC operation. *P* value: Student's *t* test. Error bar: SEM. (*P*) Sequence alignment of *Ace2* locus from mouse, human, and rat. Peak heights indicate degree of sequence homology. Black boxes (b1–b5) are regions of high sequence homology and were further analyzed by ChIP. (*Q*) ChIP-qPCR analysis of *Ace2* promoter using antibodies against Brg1 (J1 antibody) and hearts 7 d after sham or TAC operation. *P* value: Student's *t* test. Error bar: SEM. (*R*) Luciferase reporter assays of the *Ace* (−2,983 to +174 bp) and *Ace2* (−7,063 to +786 bp) proximal promoter in mouse cardiac endothelial cells. *P* value: Student's *t* test. Error bar: SEM.

anti-Brg1 antibody (34) showed that, in TAC-operated hearts Brg1 was highly enriched in three of a1–a4 regions (a2, a3, and a4), compared with the sham-operated hearts (Fig. 3O). Additionally, we analyzed the 5.5-kb upstream region of the mouse *Ace2* promoter, which contained five highly conserved regions among different species (b1–b5 in Fig. 3P). ChIP analysis of the TAC-stressed heart ventricles showed that Brg1 was highly enriched in three of the b1–b5 regions (b2, b3, and b4), compared with the sham-operated hearts (Fig. 3Q). These ChIP studies of stressed hearts indicate that Brg1, once activated by stress, binds to evolutionarily conserved regions of *Ace* and *Ace2* proximal promoters.

We next tested the transcriptional activity of Brg1 on *Ace* and *Ace2* promoters. We cloned *Ace* upstream promoter ($-2,983$ to $+174$ bp) and *Ace2* upstream promoter ($-7,063$ to $+786$ bp) into the episomal reporter pREP4 that allows promoter chromatinization in mammalian cells (24, 35). We then transfected the reporter and Brg1-expressing plasmids into mouse cardiac (coronary) endothelial cells for reporter assays (36). In these cells Brg1 caused 1.7-fold increase in *Ace* promoter activity and 59% reduction in *Ace2* promoter activity (Fig. 3R). These reporter studies, combined with the ChIP results, indicate that Brg1 activates the *Ace* promoter and represses the *Ace2* promoter. This finding provides a molecular explanation for the antithetical changes of *Ace* and *Ace2* in stressed hearts.

Endothelial FoxM1 Is Required for Stress-Induced Cardiac Hypertrophy and Pathological Ace/Ace2 Switch. We next hypothesized that FoxM1 (a forkhead box transcription factor) was the transcription factor that worked with Brg1 to antithetically regulate *Ace* and *Ace2* expression and contribute to cardiac hypertrophy. This hypothesis was based on the following observations. First, FoxM1 regulates the expression of genes associated with pathological hypertrophy (37, 38). Second, the FoxM1 protein contains both transactivation and repressor domains, capable of functioning as a transcription activator or repressor (25–27). Third, we found that FoxM1 had expression dynamics in fetal, normal adult, and stressed adult hearts, similar to that of Brg1. RT-qPCR and immunostaining of heart ventricles showed that FoxM1 was abundant in fetal hearts (Fig. S6A), but its expression was down-regulated in normal adult hearts. In contrast, in TAC-stressed hearts, FoxM1 mRNA increased by 8.4-fold (Fig. 4A), and the proteins were up-regulated in the nuclei of both cardiomyocytes and endothelial cells of stressed hearts (Fig. 4 B and C and Fig. S6 B and C). Western blot analysis of isolated cardiac endothelial cells and cardiomyocytes showed that FoxM1 protein was up-regulated by 2.5- and 2.3-fold after stress (Fig. 4 D and E and Fig. S6 D and E).

We then tested the necessity of FoxM1 activation for cardiac hypertrophy by using the FoxM1 inhibitor thiostrepton (39, 40) in TAC-stressed hearts. Within 4 wk after TAC, the control mice injected with the vehicle (DMSO) developed severe cardiac hypertrophy with increased ventricle–body weight ratio, interstitial fibrosis, and cardiac dysfunction with reduced left ventricular FS (Fig. 4 F–I). In contrast, thiostrepton-treated mice exhibited mild cardiac hypertrophy (Fig. 4F), mild interstitial fibrosis (Fig. 4 G and H), and a lesser degree of cardiac dysfunction (Fig. 4I). There was a ~50% reduction of hypertrophy and 28% improvement of FS, comparable to the improvement observed in endothelial *Brg1*-null hearts (Fig. 2 F and J). In addition, Western blot analysis of heart ventricles showed that TAC-induced Ace and Ace2 switches were abolished when FoxM1 was inhibited by thiostrepton, with the Ace/Ace2 ratio reduced by 6.5-fold in stressed hearts (Fig. 4 J and K). This finding suggests that FoxM1 is required for pathological switch of Ace and Ace2.

To test the genetic role of *FoxM1* in endothelial cells, we crossed *SclCre^ERT* mice (31) with mice that carried floxed *FoxM1* alleles (41) to generate the *SclCre^ERT;FoxM1^{fl/fl}* mouse line. This line enabled tamoxifen-induced deletion of *FoxM1* in endothelial cells. In tamoxifen-treated, TAC-operated *SclCre^ERT;FoxM1^{fl/fl}*

hearts, FoxM1 protein was absent in endothelial cells, but not in cardiomyocytes (Fig. 4 L and M), indicating an endothelial knockout of FoxM1. Within four weeks after TAC, *SclCre^ERT;FoxM1^{fl/fl}* mice displayed ~50% reduction of cardiac mass (ventricular/body weight ratio reduced from 68% to 36%, $P < 0.01$) (Fig. 4N) and ~55% reduction of cardiomyocyte size measured by WGA staining (from 69% to 31%, $P < 0.01$) (Fig. S6 F–J). Also, *SclCre^ERT;FoxM1^{fl/fl}* mice
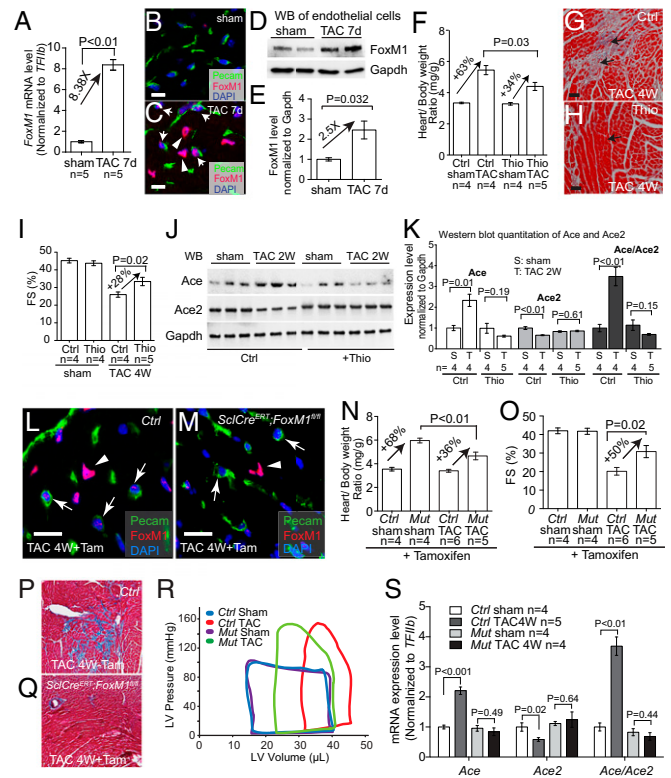

Fig. 4. Endothelial FoxM1 is essential for cardiac hypertrophy and pathological switch of Ace/Ace2. (A) Quantitation of *FoxM1* mRNA in mouse hearts after 7 d after sham or TAC operation. (B and C) Coimmunostaining of FoxM1 (red) and Pecam (green) in mouse hearts 7 d after sham or TAC operation. Arrows, endothelial cell nuclei; arrowheads, myocardial cell nuclei. (Scale bars, 10 μm.) (D and E) Western blot analysis (D) and quantitation (E) of FoxM1 proteins in cardiac endothelial cells isolated from mouse hearts 7 d after sham or TAC operation. P value: Student's t test. Error bar: SEM. (F) Quantitation of ventricle–body weight ratio of mice treated with DMSO (Ctrl) and thiostrepton (Thio) after 4 wk of sham or TAC operation. (G and H) Trichrome staining of cardiac fibrosis in mice treated with DMSO (Ctrl) and thiostrepton (Thio) after 4 wk sham or TAC operation. Red, cardiomyocytes; blue, fibrosis. Arrow, interstitial space. (Scale bars, 20 μm.) (I) Echocardiographic measurement of FS of the LV after 4 wk (4W) of TAC. Ctrl, DMSO; Thio, thiostrepton. (J and K) Western blot analysis (J) and quantitation (K) of Ace and Ace2 proteins in the heart of DMSO-treated (Ctrl) and thiostrepton-treated (Thio) mice 2 wk (2W) after sham or TAC operation. (L and M) Coimmunostaining of FoxM1 (red) and Pecam (green) in control (Ctrl) and *SclCre^ERT;FoxM1^{fl/fl}* mouse hearts 4 wk after TAC operation with tamoxifen treatment. Arrows, endothelial cell nuclei; arrowheads, myocardial cell nuclei. (Scale bars, 10 μm.) (N) Quantitation of ventricle–body weight ratio in control (Ctrl) and *SclCre^ERT;FoxM1^{fl/fl}* (Mut) mice 4 wk after sham or TAC operation. P value: Student's t test. Error bar: SEM. (O) Echocardiographic measurement of FS of the left ventricle of control (Ctrl) and *SclCre^ERT;FoxM1^{fl/fl}* (Mut) hearts after 4 wk of TAC. P value: Student's t test. Error bar: SEM. (P and Q) Trichrome staining of cardiac fibrosis in control (P) and *SclCre^ERT;FoxM1^{fl/fl}* (Q) mice 4 wk after sham or TAC operation. Original magnification: 200×. Red, cardiomyocytes; blue, fibrosis. (R) Representative LV pressure–volume (PV) loops taken after cardiac catheterization of control (Ctrl) and *SclCre^ERT; FoxM1^{fl/fl}* (Mut) mice 4 wk after sham or TAC operation. (S) Quantitation of *Ace*, *Ace2*, and *Ace/Ace2* mRNA in control (Ctrl) and *SclCre^ERT;FoxM1^{fl/fl}* (Mut) heart ventricles after sham or TAC operation. P value: Student's t test. Error bar: SEM.
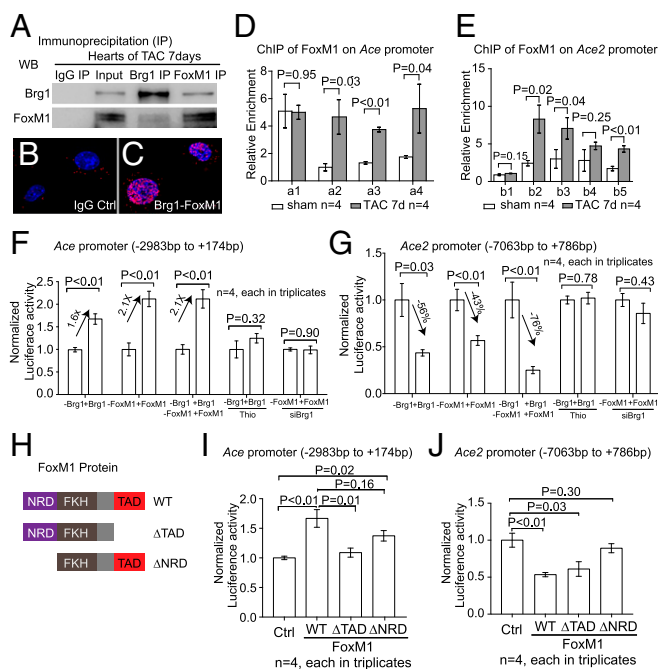
Fig. 5. Brg1 cooperates with FoxM1 to control *Ace* and *Ace2* expression. (*A*) Coimmunoprecipitation of Brg1 with FoxM1 in heart ventricles after 7 d of TAC. (*B* and *C*) Proximity ligation assay of Brg1–FoxM1 complex in nuclei of cultured mouse cardiac endothelial cells. Original magnification: 400×. Red, proximity ligation signal; blue, DAPI. IgG control, cells treated with IgG but not primary anti-Brg1 or -FoxM1 antibodies. (*D* and *E*) ChIP-qPCR analysis of *Ace* (*D*) and *Ace2* (*E*) promoters using antibodies against FoxM1 7 d after sham or TAC operation. (*F* and *G*) Luciferase reporter assays of the *Ace* (−2,983 to +174 bp) (*F*) and *Ace2* (−7,063 to +786 bp) (*G*) proximal promoters (described in Fig. 3 *L* and *N*) in mouse cardiac endothelial cells. siBrg1, siRNA-mediated knockdown of Brg1; Thio, thiostrepton. *P* value: Student's *t* test. Error bar: SEM. (*H*) Schematic illustration of FoxM1 repression, trans-activation domains, and mutations. NRD, N-terminal repression domain; TAD, C-terminal transactivation domain. (*I* and *J*) Luciferase reporter assays of the *Ace* (*I*) and *Ace2* (*J*) promoters with FoxM1 mutants in mouse cardiac endothelial cells. *P* value: Student's *t* test. Error bar: SEM.

showed ∼50% improvement of left ventricular FS by echocardiography (*P* = 0.02) (Fig. 4*O*) and a dramatic reduction of stress-induced interstitial fibrosis (Fig. 4 *P* and *Q*). A complete characterization of heart function by cardiac catheterization further validated that endothelial *FoxM1* deletion greatly improved the function of TAC-stressed hearts (Fig. 4*R*). Endothelial *FoxM1* deletion improved EF of the stressed hearts by 49%, SV by 32%, CO by 28%, and plPwr by 54% (Fig. S7 *A–D*). The left ventricular ESV was reduced by 32% (*P* < 0.01), and end-diastolic volume was reduced by 11% (*P* = 0.03). The stress-induced changes of diastolic relaxation (Tau) were reduced by 34% (Fig. S7 *E–G*), and the left ventricular filling pressure (EDP) was reduced by 38% (*P* < 0.01) (Fig. S7*H*). These findings indicate that endothelial FoxM1 disruption prevents the development of cardiac dysfunction in stressed hearts. Furthermore, the TAC-induced pathological Ace/Ace2 switch was abolished with Ace/Ace2 ratio normalized in those hearts lacking endothelial FoxM1 (Fig. 4*S*). These findings indicate that activation of endothelial FoxM1 expression is essential for stress-induced cardiac hypertrophy and the pathological *Ace/Ace2* switch.

Brg1 Cooperates with FoxM1 in the Endothelium to Control Cardiac *Ace* and *Ace2* Expression. Given that both FoxM1 and Brg1 could regulate Ace/Ace2 switch in stressed cardiac endothelium, we tested whether there was a direct physical interaction between these two proteins. We found that Brg1 coimmunoprecipitated

with FoxM1 in stressed heart ventricles (Fig. 5*A*). Proximity ligation (Duolink) assay (42, 43) further confirmed that Brg1 and FoxM1 formed a protein complex in the nuclei of mouse cardiac endothelial cells (Fig. 5 *B* and *C*). We then asked whether FoxM1, like Brg1, could bind to the promoters of *Ace* and *Ace2* in stressed hearts. ChIP analysis showed that FoxM1 was highly enriched in the conserved regions of *Ace* and *Ace2* proximal promoters of TAC-stressed hearts relative to the sham-operated hearts (Fig. 5 *D* and *E*). The binding pattern of FoxM1 was broadly similar to that of Brg1 (Fig. 3 *M* and *O*). Given that DNA elements could be looped and brought together by proteins bound to them and that Brg1 and FoxM1 formed a physical complex in stressed endothelial cells, the results suggest that Brg1 and FoxM1 form a protein complex on *Ace* and *Ace2* promoters to orchestrate regulatory DNA elements to control *Ace* and *Ace2* expression. Furthermore, luciferase reporter assays conducted in mouse cardiac endothelial cells showed that FoxM1, like Brg1, was capable of activating *Ace* and repressing *Ace2* promoter activities (Fig. 5 *F* and *G*). Inhibition of FoxM1 by thiostrepton (39, 40) eliminated Brg1-mediated *Ace* promoter activation and *Ace2* promoter repression (Fig. 5 *F* and *G*). Likewise, knockdown of Brg1 abolished FoxM1's activity on *Ace* activation and *Ace2* repression (Fig. 5 *F* and *G*). These results indicate that Brg1 and FoxM1 are mutually dependent for the regulation of *Ace* and *Ace2* promoters. To determine whether FoxM1 used different effector domains to control *Ace* and *Ace2* expression, we constructed two mutated
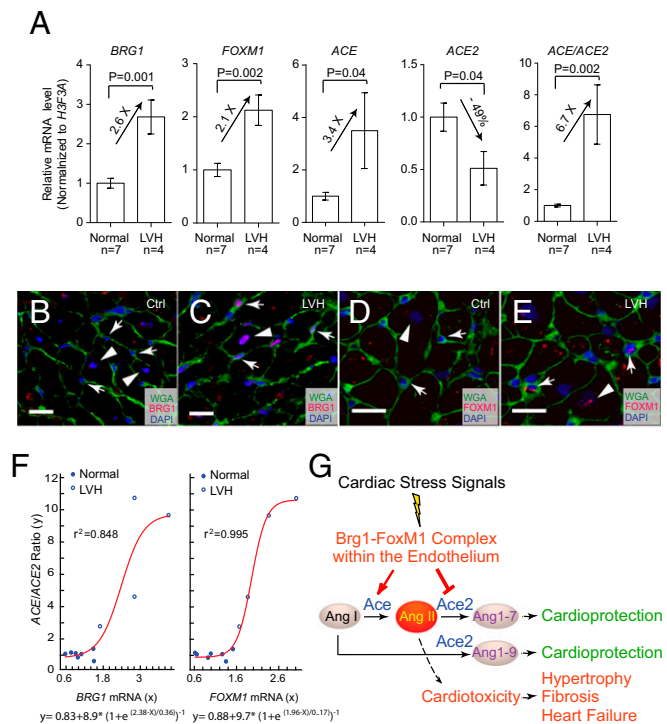

Fig. 6. BRG1 and FOXM1 activation in human cardiomyopathy. (*A*) qPCR analysis of *BRG1*, *FOXM1*, *ACE*, and *ACE2* expression and *ACE/ACE2* ratio in normal (*n* = 7) and LVH hearts (*n* = 4). (*B* and *C*) Coimmunostaining of BRG1 (red) and WGA (green) in normal and LVH hearts. Arrow, endothelial cell; arrowhead, myocardial cell. (Scale bars, 10 μm.) (*D* and *E*) Coimmunostaining of FOXM1 (red) and WGA (green) in heart of normal and LVH subjects. Arrow, endothelial cell; arrowhead, myocardial cell. (Scale bars, 10 μm.) (*F*) Correlation of *BRG1* and *FOXM1* mRNA level (*x* axis) with *ACE/ACE2* mRNA ratio (*y* axis), *n* = 11. Red, nonlinear regression curve. e, the base of natural logarithm (∼2.718). Equations of Boltzmann sigmoidal model are listed under the graphs. (*G*) Working model of how cardiac endothelial Brg1–FoxM1 complex mediates stress signals to control Ace/Ace2 and angiotensin production in the heart.

FoxM1 proteins: FoxM1 with C-terminal transactivation domain truncated (ΔTAD) and FoxM1 with N-terminal repression domain truncated (ΔNRD) (refs. 44 and 45 and Fig. 5H). Without the transactivation domain, the FoxM1–ΔTAD mutants failed to activate the *Ace* promoter, but maintained its repression of the *Ace2* promoter (Fig. 5 I and J). Conversely, without the repressor domain, FoxM1–ΔNRD mutants failed to repress the *Ace2* promoter, but preserved effects on *Ace* promoter activation (Fig. 5 I and J). These results indicate that FoxM1 functions through different transcriptional effector domains for the regulation of *Ace* and *Ace2* promoters, providing a molecular explanation for the antithetical effects of the Brg1–FoxM1 complex on *Ace* and *Ace2*. Overall, the ChIP and reporter analyses, combined with the stress-induced formation of the Brg1–FoxM1 complex, suggest that Brg1 and FoxM1 cooperate to regulate the pathological switch of *Ace* and *Ace2* in the stressed heart.

Implications for Human Cardiac Hypertrophy. To investigate whether *BRG1* and *FOXM1* were also activated in the endothelial cells of human hypertrophic hearts, we studied patients with left ventricular hypertrophy (LVH). The tissue samples were obtained from donor hearts that were considered unsuitable for transplantation because of the lack of timely recipients or mismatched surgical cut (Fig. S8). RT-qPCR of mRNA showed that the human hypertrophic hearts had a 2.1- and 2.6-fold increase of *FOXM1* and *BRG1*, a 3.4-fold increase of *ACE*, and a 51% reduction of *ACE2*, with the *ACE/ACE2* ratio increased by 6.7-fold (Fig. 6A). Like in mice, BRG1 and FOXM1 were up-regulated in both cardiomyocytes and endothelial cells of the hypertrophic hearts (Fig. 6 B–E). Nonlinear regression analysis showed that the level of BRG1 and FOXM1 correlated strongly with the level of pathological switch of ACE/ACE2 in human hearts (Fig. 6F; $r^2 = 0.848$ and 0.995, respectively). The human tissue studies thus suggest an evolutionarily conserved mechanism underlying myopathy of mouse and human hearts.

Discussion

Controlling Ace/Ace2 expression is critical for maintaining cardiac function, given that an increase of Ace or reduction of Ace2 is sufficient to cause cardiomyopathy (20, 23, 46). We showed that the Ace and Ace2 amount in the heart is controlled primarily at the transcription level and identified an endothelial chromatin complex composed of Brg1 and FoxM1 that transcriptionally activates *Ace* and represses *Ace2* in response to cardiac stress (Fig. 6G). This finding provides new molecular insights into endothelial–myocardial interaction under pathological conditions. The requirement of the Brg1–FoxM1 complex for pathological hypertrophy has important implications for heart failure therapy. In stressed hearts, a chemical inhibitor of FoxM1 is effective in reversing Ace/Ace2 and preventing cardiac hypertrophy and dysfunction. It is therefore pharmacologically feasible to inhibit Ace and activate Ace2 simultaneously to improve heart function. Given that there has not been an effective chemical activator of Ace2, likely because of the difficulty of generating protein activators of any kind, chemical inhibition of Brg1–FoxM1 complex reveals a new avenue for pharmacologically targeting *Ace* and *Ace2* genes simultaneously to reverse Ace/Ace2 ratio in failing hearts. Besides *Ace/Ace2* regulation, broader functions of the endothelial Brg1–FoxM1 complex will require a future genome-wide approach to determine other downstream targets of this complex in stressed hearts.

At the molecular level, Brg1 and FoxM1 interactions show a molecular mechanism for Brg1 and FoxM1 in gene regulation. The FoxM1 protein contains both a transactivating and a repressor domain for transcription regulation. How such dual transcription activity of FoxM1 is controlled remains unclear. We showed here that Brg1 is essential for FoxM1 to repress *Ace* and to activate *Ace2*. However, it remains unknown how Brg1 enables FoxM1 to use its repressor domain on one promoter (such as *Ace*) and its transactivating domain on another promoter (such as *Ace2*). Such promoter-specific activity of FoxM1 may be caused by how Brg1 rearranges the chromatin–DNA for FoxM1 to bind or by other unidentified factors in the promoter that differentially expose or enable the FoxM1 transactivating or repressor domain. Given that FoxM1 is required for embryogenesis and is a proto-oncogene up-regulated in many human cancers, including lung, breast, and colon cancers (25–27, 47), future studies to define the molecular details of the differential domain use of FoxM1 may have important implications in organ development, cardiac hypertrophy, and many other diseases.

Materials and Methods

*Brg1^fl/fl^*, *FoxM1^fl/fl^*, and *SclCre^ERT^* [endothelial-SCL-Cre-ERT (31)] mice have been described (32, 48–50). Littermate CD1 male mice were purchased from Charles River (strain code 022). Animal use protocol was reviewed and approved by Indiana University Institutional Animal Care and Use Committee (IACUC). Only de-identified human tissues were used for studies. The human tissues were processed for RT-qPCR. The use of human tissues is in compliance with the regulation of Sanford/Burnham Medical Research Institute and Indiana University. Informed consent procedures were in compliance with Institutional Biosafety Committee protocol (no. 1784) approved by Indiana University. Curve modeling was performed with the Levenburg–Marquardt nonlinear regression method and XLfit software.

Additional materials and procedures are provided in *SI Materials and Methods*.

1. Mozaffarian D, et al.; American Heart Association Statistics Committee and Stroke Statistics Subcommittee (2015) Heart disease and stroke statistics—2015 update: A report from the American Heart Association. *Circulation* 131(4):e29–e322.

2. Canetti M, et al. (2003) Evaluation of myocardial blood flow reserve in patients with chronic congestive heart failure due to idiopathic dilated cardiomyopathy. *Am J Cardiol* 92(10):1246–1249.

3. Dini FL, et al. (2009) Coronary flow reserve in idiopathic dilated cardiomyopathy: Relation with left ventricular wall stress, natriuretic peptides, and endothelial dysfunction. *J Am Soc Echocardiogr* 22(4):354–360.

4. Bitar F, et al. (2006) Variable response of conductance and resistance coronary arteries to endothelial stimulation in patients with heart failure due to nonischemic dilated cardiomyopathy. *J Cardiovasc Pharmacol Ther* 11(3):197–202.

5. Mathier MA, et al. (1998) Coronary endothelial dysfunction in patients with acute-onset idiopathic dilated cardiomyopathy. *J Am Coll Cardiol* 32(1):216–224.

6. Elesber AA, et al. (2007) Coronary endothelial dysfunction and hyperlipidemia are independently associated with diastolic dysfunction in humans. *Am Heart J* 153(6):1081–1087.

7. Shantsila E, Wrigley BJ, Blann AD, Gill PS, Lip GY (2012) A contemporary view on endothelial function in heart failure. *Eur J Heart Fail* 14(8):873–881.

8. Paul M, Poyan Mehr A, Kreutz R (2006) Physiology of local renin-angiotensin systems. *Physiol Rev* 86(3):747–803.

9. Lindpaintner K, et al. (1988) Intracardiac generation of angiotensin and its physiologic role. *Circulation* 77(6 Pt 2):I18–I23.

10. Danser AH, et al. (1994) Cardiac renin and angiotensins. Uptake from plasma versus in situ synthesis. *Hypertension* 24(1):37–48.

11. Dell'Italia LJ, et al. (1997) Compartmentalization of angiotensin II generation in the dog heart. Evidence for independent mechanisms in intravascular and interstitial spaces. *J Clin Invest* 100(2):253–258.

12. Heller LJ, Opsahl JA, Wernsing SE, Saxena R, Katz SA (1998) Myocardial and plasma renin-angiotensinogen dynamics during pressure-induced cardiac hypertrophy. *Am J Physiol* 274(3 Pt 2):R849–R856.

13. van Kats JP, et al. (1998) Angiotensin production by the heart: A quantitative study in pigs with the use of radiolabeled angiotensin infusions. *Circulation* 98(1):73–81.

14. de Lannoy LM, et al. (1997) Renin-angiotensin system components in the interstitial fluid of the isolated perfused rat heart. Local production of angiotensin I. *Hypertension* 29(6):1240–1251.

15. Falkenhahn M, et al. (1995) Cellular distribution of angiotensin-converting enzyme after myocardial infarction. *Hypertension* 25(2):219–226.

16. Vickers C, et al. (2002) Hydrolysis of biological peptides by human angiotensin-converting enzyme-related carboxypeptidase. *J Biol Chem* 277(17):14838–14843.

17. Ocaranza MP, et al. (2010) Angiotensin-(1-9) regulates cardiac hypertrophy in vivo and in vitro. *J Hypertens* 28(5):1054–1064.

18. Loot AE, et al. (2002) Angiotensin-(1-7) attenuates the development of heart failure after myocardial infarction in rats. *Circulation* 105(13):1548–1550.

19. Silva GJ, et al. (2006) ACE gene dosage modulates pressure-induced cardiac hypertrophy in mice and men. *Physiol Genomics* 27(3):237–244.

20. Zhong J, et al. (2010) Angiotensin-converting enzyme 2 suppresses pathological hypertrophy, myocardial fibrosis, and cardiac dysfunction. Circulation 122(7):717–728.

21. Epelman S, et al. (2008) Detection of soluble angiotensin-converting enzyme 2 in heart failure: Insights into the endogenous counter-regulatory pathway of the renin-angiotensin-aldosterone system. *J Am Coll Cardiol* 52(9):750–754.

22. Mehta PK, Griendling KK (2007) Angiotensin II cell signaling: Physiological and pathological effects in the cardiovascular system. *Am J Physiol Cell Physiol* 292(1):C82–C97.

23. Crackower MA, et al. (2002) Angiotensin-converting enzyme 2 is an essential regulator of heart function. *Nature* 417(6891):822–828.

24. Hang CT, et al. (2010) Chromatin regulation by Brg1 underlies heart muscle development and disease. *Nature* 466(7302):62–67.

25. Kalin TV, Ustiyan V, Kalinichenko VV (2011) Multiple faces of FoxM1 transcription factor: lessons from transgenic mouse models. *Cell Cycle* 10(3):396–405.

26. Bella L, Zona S, Nestal de Moraes G, Lam EW (2014) FOXM1: A key oncofoetal transcription factor in health and disease. *Semin Cancer Biol* 29:32–39.

27. Wierstra I (2013) The transcription factor FOXM1 (Forkhead box M1): Proliferation-specific expression, transcription factor function, target genes, mouse models, and normal biological roles. *Adv Cancer Res* 118:97–398.

28. Han P, et al. (2014) A long noncoding RNA protects the heart from pathological hypertrophy. *Nature* 514(7520):102–106.

29. Brutsaert DL (2003) Cardiac endothelial-myocardial signaling: Its role in cardiac growth, contractile performance, and rhythmicity. *Physiol Rev* 83(1):59–115.

30. Dong QG, et al. (1997) A general strategy for isolation of endothelial cells from murine tissues. Characterization of two endothelial cell lines from the murine lung and subcutaneous sponge implants. *Arterioscler Thromb Vasc Biol* 17(8):1599–1604.

31. Göthert JR, et al. (2004) Genetically tagging endothelial cells in vivo: Bone marrow-derived cells do not contribute to tumor endothelium. *Blood* 104(6):1769–1777.

32. Sumi-Ichinose C, Ichinose H, Metzger D, Chambon P (1997) SNF2beta-BRG1 is essential for the viability of F9 murine embryonal carcinoma cells. *Mol Cell Biol* 17(10):5976–5986.

33. Sano M, et al. (2007) p53-induced inhibition of Hif-1 causes cardiac dysfunction during pressure overload. *Nature* 446(7134):444–448.

34. Stankunas K, et al. (2008) Endocardial Brg1 represses ADAMTS1 to maintain the microenvironment for myocardial morphogenesis. *Dev Cell* 14(2):298–311.

35. Liu R, et al. (2001) Regulation of CSF1 promoter by the SWI/SNF-like BAF complex. *Cell* 106(3):309–318.

36. Barbieri SS, Weksler BB (2007) Tobacco smoke cooperates with interleukin-1beta to alter beta-catenin trafficking in vascular endothelium resulting in increased permeability and induction of cyclooxygenase-2 expression in vitro and in vivo. *FASEB J* 21(8):1831–1843.

37. Hannenhalli S, et al. (2006) Transcriptional genomics associates FOX transcription factors with human heart failure. *Circulation* 114(12):1269–1276.

38. Song HK, Hong SE, Kim T, Kim H (2012) Deep RNA sequencing reveals novel cardiac transcriptomic signatures for physiological and pathological hypertrophy. *PLoS One* 7(4):e35552.

39. Bhat UG, Halasi M, Gartel AL (2009) Thiazole antibiotics target FoxM1 and induce apoptosis in human cancer cells. *PLoS One* 4(5):e5592.

40. Hegde NS, Sanders DA, Rodriguez R, Balasubramanian S (2011) The transcription factor FOXM1 is a cellular target of the natural product thiostrepton. *Nat Chem* 3(9):725–731.

41. Krupczak-Hollis K, et al. (2004) The mouse Forkhead Box m1 transcription factor is essential for hepatoblast mitosis and development of intrahepatic bile ducts and vessels during liver morphogenesis. *Dev Biol* 276(1):74–88.

42. Söderberg O, et al. (2006) Direct observation of individual endogenous protein complexes in situ by proximity ligation. *Nat Methods* 3(12):995–1000.

43. Fredriksson S, et al. (2002) Protein detection using proximity-dependent DNA ligation assays. *Nat Biotechnol* 20(5):473–477.

44. Fu Z, et al. (2008) Plk1-dependent phosphorylation of FoxM1 regulates a transcriptional programme required for mitotic progression. *Nat Cell Biol* 10(9):1076–1082.

45. Park HJ, et al. (2008) An N-terminal inhibitory domain modulates activity of FoxM1 during cell cycle. *Oncogene* 27(12):1696–1704.

46. Yusuf S, et al.; The Heart Outcomes Prevention Evaluation Study Investigators (2000) Effects of an angiotensin-converting-enzyme inhibitor, ramipril, on cardiovascular events in high-risk patients. *N Engl J Med* 342(3):145–153.

47. Radhakrishnan SK, Gartel AL (2008) FOXM1: The Achilles' heel of cancer? *Nat Rev Cancer* 8(3):c1; author reply c2.

48. Tachibana M, Nozaki M, Takeda N, Shinkai Y (2007) Functional dynamics of H3K9 methylation during meiotic prophase progression. *EMBO J* 26(14):3346–3359.

49. Thomas LR, et al. (2008) Functional analysis of histone methyltransferase g9a in B and T lymphocytes. *J Immunol* 181(1):485–493.

50. Wu B, et al. (2010) Inducible cardiomyocyte-specific gene disruption directed by the rat Tnnt2 promoter in the mouse. *Genesis* 48(1):63–72.

51. Chang CP, et al. (2004) A field of myocardial-endocardial NFAT signaling underlies heart valve morphogenesis. *Cell* 118(5):649–663.

52. Trivedi CM, et al. (2007) Hdac2 regulates the cardiac hypertrophic response by modulating Gsk3 beta activity. *Nat Med* 13(3):324–331.

53. Khavari PA, Peterson CL, Tamkun JW, Mendel DB, Crabtree GR (1993) BRG1 contains a conserved domain of the SWI2/SNF2 family necessary for normal mitotic growth and transcription. *Nature* 366(6451):170–174.